

STUDY OF THE ELECTRON SEEDED PROTON SELF-MODULATION USING FBPIC

L. Liang^{*1}, G. Xia¹, University of Manchester, Manchester, United Kingdom

A. Bonatto, Universidade Federal de Ciências da Saúde de Porto Alegre, Porto Alegre, Brazil

¹also at Cockcroft Institute, Daresbury, United Kingdom

Abstract

In order to make a full use of the whole proton bunch to drive large amplitude plasma wakefields and suppress the uncontrolled growth of any possible instabilities at the head of the proton bunch, the AWAKE Run 2 experiment plans to use an electron bunch to seed the formation of the proton bunch self-modulation. Additionally, a density step in the plasma channel will be used to freeze the self-modulation process to keep the wakefield amplitude. In this work, numerical simulations performed with FBPIC are used to investigate the electron seeded proton self-modulation and the effect of the plasma density step as well.

INTRODUCTION

The particle beam driven plasma wakefield acceleration (PWFA) has shown the ability to generate ultra-high accelerating gradients (>50 GV/m), which far exceeds those in radio-frequency accelerators [1]. Since effectively exciting plasma wave requires a driver beam with a length on the order of the plasma wavelength λ_{pe} , the Advanced Wakefield Experiment (AWAKE) at CERN exploited the seeded self-modulation (SSM) technique to transform a long proton bunch into a train of short bunches, then accelerated an externally injected electron bunch to 2 GeV in the proton driven wakefields [2].

The seeding field of the self-modulation in AWAKE Run 1 is provided by the laser-formed relativistic ionization front (RIF) located in the middle of the proton bunch, which can only seed the controlled self-modulation of protons after the ionization front [3]. Uncontrollable self-modulation instability (SMI) may grow in the front part when the proton bunch with an unmodulated head propagates further in a preformed plasma channel. This effect can be destructive for the wakefield stability and hence the reproducibility of the electron acceleration. Thus in AWAKE Run 2, the electron bunch seeding method, which could lead to self-modulation of the entire bunch, is adopted [3].

Another problem that could prevent the wakefield from growing in the SSM process is the dephasing of plasma wave with respect to (w.r.t) the proton micro bunch [4]. The large phase shift will force a large fraction of those micro bunches into the defocusing phase, which then leads to dramatic proton loss and hence wake amplitude decrease after reaching the peak. By using a plasma profile with a ramped-up density step [5], the SSM process can be slowed down, and the

large accelerating gradient can be maintained over longer distance.

The SSM study in previous publications [5, 6] is mainly performed by the quasi-static particle-in-cell (PIC) codes, e.g. LCODE [7], which assumes the beam envelope evolves slowly as it propagates in plasmas. In this proceeding, we use FBPIC [8], a spectral, quasi-3D full PIC code without physical approximations, to take a further look at the electron seeded self-modulation and cross-check it with other results.

CONFIGURATIONS

Typical proton beam and plasma parameters of the AWAKE experiment can be found in [6]. Due to the limitation of computing resource, the RMS length of the proton beam and the number of particles per bunch are scaled down by ten times to $\sigma_{zp} = 7$ mm and $N_p = 3 \times 10^{10}$, respectively. The proton beam has a nominal energy of $E_{p0} = 400$ GeV, a relative energy spread of $\Delta E_{p0}/E_{p0} = 0.035\%$ and a RMS transverse radius of $\sigma_{rp} = 0.2$ mm. The baseline parameters of preceding electron beam that is used to drive the seeding wakefields (referred as seed beam hereafter) are beam energy $E_{e0} = 18$ MeV, relative energy spread $\Delta E_{e0}/E_{e0} = 0.1\%$, RMS length $\sigma_{ze} = 0.3$ mm, RMS transverse radius $\sigma_{re} = 0.2$ mm and charge $Q_e = 0.5$ nC. One should notice that the seed beam parameters chosen here can be a bit of different with that in [6], especially the RMS seed beam length σ_{ze} . It was chosen to let the whole seed beam reside in the decelerating phase so as to deplete the seed beam and remove it from the plasma much faster [9]. The proton beam and seed beam are represented by 10^6 and 10^5 macroparticles in the simulation box, respectively. The seed beam is aligned with the proton beam on the z -axis, with a space of $4.5\sigma_{zp}$ between the two bunches. The nominal density of the pre-ionized Rubidium plasma is $n_0 = 2 \times 10^{14}$ cm⁻³ (the low density case of AWAKE Run 2 [6]) and the length of the plasma cell is assumed to be $L_p = 10$ m. The plasma column has a finite transverse radius of $r_{pe} = 1.6$ mm = $8\sigma_{zp}$.

The simulation window moves with a speed close to that of the light ($\sim c$) in the beam propagation direction. To ensure transverse physical effects are correctly simulated [10], the radial size r_w of the longitudinally-axisymmetric simulation box is set as two times r_{pe} , i.e. $r_w = 3.2$ mm, as shown in Fig. 1. A transverse grid cell size of $\Delta r = 4$ μ m, and of $\Delta z = 8$ μ m for the longitudinal grid cells is used to resolve the particle motion and wakefields. The number of plasma particles per cell is set to be 2 along the coordinate z and 6 along the coordinate r . $\xi = z - ct$ represents the longitudinal

* linbo.liang@postgrad.manchester.ac.uk

coordinate in the simulation window, with $s = ct$ being the co-moving distance w.r.t the lab frame.

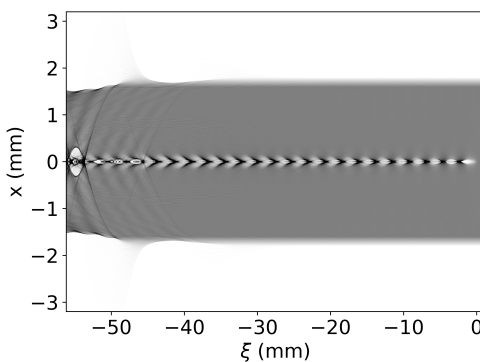


Figure 1: Plasma electron density distribution at $s = 0.4$ m.

RESULTS

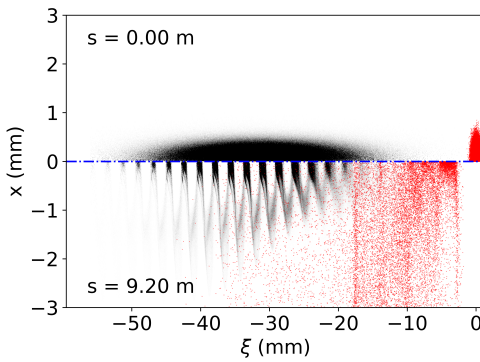


Figure 2: Simulation-obtained proton density (black) and electron macroparticle (red) distribution plot at the beginning (up-half, $s = 0$ m) and after self-modulation (down-half, $s = 9.2$ m). Longitudinal plasma profile: Uniform.

The simulation study is started with the longitudinally-uniform plasma density profile at first. Figure 2 shows the simulated density of the proton beam (black shade) and the distribution of the electron macro-particles (red dots) of the uniform plasma profile case. While the upper half of Fig. 2 corresponds to the particle distribution at the beginning of the simulation, the lower half represents it at a propagation distance of $s = 9.2$ m. One can see that the initial long proton bunch is modulated into about 15 quasi-equally-spaced micro-bunches. Protons between these dense micro-bunches and also different fraction of protons that were supposed to be in these micro-bunches are deflected outwards by the transverse defocusing force. Micro-bunches are obviously thinner in longitudinal direction towards the tail. This is caused by the phase-shift between the wakefields and proton-bunches, as aforementioned. As a result, the established accelerating gradient (for electron witness) largely decreases after reaching the peak, as shown by the blue solid line (no marker) in Fig. 3. As for the seed beam, it is quickly depleted in the

first half meter, which causes a moderate amplitude drop of the accelerating gradient in the first meter before the fast growth of SSM. Then the whole bunch slippes backwards w.r.t the proton beam from its initial position and spreads over a quite large phase. Meanwhile, the down-half plot of Fig. 2 as well as the statistical results show that more than 80% of these electrons are also expelled out radially by the transverse defocusing force.

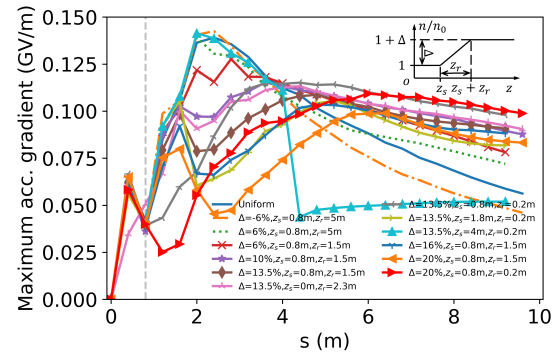


Figure 3: The maximum accelerating gradient for distinct plasma density profiles. The vertical dashed line marks $s = 0.8$ m. The insert at the upper-right corner shows the schematic layout of the plasma density step.

Figure 4 shows the evolution map of the longitudinal wakefield E_z that is measured on the z -axis along the beam and w.r.t the beam propagation distance s . One obvious feature in Fig. 4 is that the seed wakefield amplitude is soon damped after the seed beam is depleted while the wakefield driven by proton micro-bunches starts to grow and dominate in the back-half of the simulation window ($\xi < -30$ mm). However, after reaching the peak at around $s = 2$ m, the proton-driven wakefield gets gradually weaker. Along with the change of field amplitude is the phase shift of the zero-field points, which are marked by black lines in Fig. 4. They have been significantly moving towards the beam head after propagating 8 meters in the plasma as a consequence of the micro-bunch destruction. Also due to this phase shift, the partially destroyed micro-bunches first fall into the even stronger focusing region, then to a weaker focusing phase, and finally to the defocusing region, which then forms a positive feedback loop and leads to the continuing process of proton loss and wakefield decay.

One might also notice that at the initial moment ($s < 1$ m), there is a phase-mixing region with unusually high field amplitude positioned at $\xi < -50$ mm in Fig. 4. This phenomenon is due to the wave-breaking induced by the trajectory crossing of returning plasma electrons, as shown in Fig. 1. These returning plasma electrons were first radially pushed out of the narrow plasma channel by the seed wakefield, then being dragged back by the restoring force due to charge separation [10]. As the singularity point of plasma electrons formed around the axis with the accumulation of returning plasma electrons, the original plasma wave structure breaks at the trajectory crossing point. The wave-breaking

effect can generate ultra-high defocusing wakefield, which could hamper the growth of the SSM. A detailed study of this effect happening in RIF seeded self-modulation can be found in [10], in which the trajectory crossing can occur several times. However, in our simulations, the re-entry point of returning plasma electrons is behind the main body of proton beam. So the wave-breaking effect does not significantly affect the SSM growth.

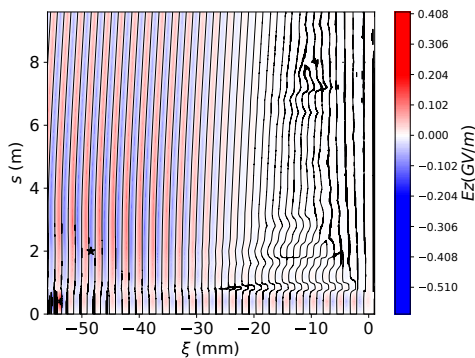


Figure 4: Evolution map of the on-axis longitudinal plasma wakefield E_z for the uniform plasma profile case. The black star marks the position where the maximum accelerating gradient is measured.

Figure 3 shows the maximum accelerating gradients obtained for distinct longitudinal plasma density profiles. The maximum accelerating gradient is measured at around $\xi = -48.5$ mm, marked by the black star in Fig. 4. For simplicity, here we only consider the linear ramp profile as shown by the insert plot, where $\Delta = \delta n/n_0$ is the relative density increase/decrease, z_s is the step starting point and z_r is the step length. Considering the optimum density increase Δ , there is a simple estimation $\Delta = \delta n/n_0 = 2/N$ for the RIF seeded case [11], where N is the number of proton micro-bunches. For the total micro bunches of $N = 15$ in the present scenario, this equation gives the estimated optimum density increase of $\Delta \approx 13.3\%$ (here we take the value of 13.5%). For the full scale SPS proton beam [6], this value can be much smaller. It is shown that the sharp ($z_r = 0.2$ m) density steps started at $z_s = 0.8$ m with relative density increase $\Delta = 13.3\%$ and 20% can both show the best effect of maintaining the accelerating gradient, and the final value is about 75% higher than that of the uniform plasma profile case. For the same density increase and step starting-point $z_s = 0.8$ m, Fig. 3 shows that a sharp plasma density has a better performance than that of a smoother step ($z_r = 1.5$ m), which is different than the findings in [6]. Other plasma profiles with positive density steps started before reaching the gradient peak can also show different extent of improvement. In contrast, the negative step ramp considered here, i.e., -6% , can only enhance the wakefield decay. As the positive density step can make the local plasma wavelength shorter than the periods of the partially-bunched micro-bunches and the increased density will act as a “spring” to resist the non-linear elongation of the wakefield period after the saturation

of SSM [11], it should start and end before the SSM reaching saturation point, where accelerating gradient peak is reached. A density step formed after the saturation point can no longer accomplish the aimed function but produce the negative effect, like the case with step start from $z_s = 4$ m.

CONCLUSION

In this proceeding, we studied the electron-seeded proton self-modulation with the quasi-3D full PIC code FBPIC. The simulation results of the scaled-down model proved the validity of this seeding method. By using a proper plasma density profile, one can effectively maintain the final accelerating gradient at a significantly higher level. These results generally agree with those from other codes. However, the ultra-high computing cost prevent us from investigating the full scale problem, for example, the possible effects due to wave-breaking induced by the returning plasma electrons to the SSM of a full length beam. Nevertheless, the available results might be useful as a reference for other simulations.

ACKNOWLEDGMENTS

The authors would like to acknowledge the support from the Cockcroft Institute Core Grant and the STFC AWAKE Run 2 grant ST/T001917/1. This work made use of the BEDE HPC of the N8 Centre of Excellence in Computationally Intensive Research (N8 CIR) provided and funded by the N8 research partnership and EPSRC (Grant No. EP/T022167/1). The authors would also like to acknowledge the assistance given by Research IT and the use of the Computational Shared Facility at The University of Manchester. The constructive discussion with Prof. Konstantin Lotov of Novosibirsk State University about the phase shift effect is also greatly appreciated.

REFERENCES

- [1] I. Blumenfeld *et al.*, “Energy doubling of 42 GeV electrons in a metre-scale plasma wakefield accelerator”, *Nature*, vol. 445, pp. 741-744, 2007. doi:10.1038/nature05538
- [2] E. Adli *et al.*, “Acceleration of electrons in the plasma wakefield of a proton bunch”, *Nature*, vol. 561, no. 7723, pp. 363-367, 2018. doi:10.1038/s41586-018-0485-4
- [3] P. Muggli *et al.*, “Seeding self-modulation of a long proton bunch with a short electron bunch”, *J. Phys. Conf. Ser.*, vol. 1596, p. 012065, Jul. 2020. doi:10.1088/1742-6596/1596/1/012066
- [4] A. Pukhov *et al.*, “Phase velocity and particle injection in a self-modulated proton-driven plasma wakefield accelerator”, *Phys. Rev. Lett.*, vol. 107, no. 14, p. 145003, 2011. doi:10.1103/PhysRevLett.107.145003
- [5] K. V. Lotov, “Controlled self-modulation of high energy beams in a plasma”, *Phys. Plasmas*, vol. 18, no. 2, 2011. doi:10.1063/1.3558697
- [6] K. V. Lotov and V. A. Minakov, “Proton beam self-modulation seeded by electron bunch in plasma with density ramp”, *Plasma Phys. Control. Fusion*, vol. 62, no. 11, p. 115025, 2020. doi:10.1088/1361-6587/abba42

- [7] A. P. Sosedkin and K. V. Lotov, “LCODE: A parallel quasistatic code for computationally heavy problems of plasma wakefield acceleration”, *Nucl. Instr. and Meth. A*, vol. 829, pp. 350-352, 2016. doi:10.1016/j.nima.2015.12.032
- [8] R. Lehe, M. Kirchen, I. A. Andriyash, B. B. Godfrey, and J.-L. Vay, “A spectral, quasi-cylindrical and dispersion-free Particle-In-Cell algorithm”, *Comput. Phys. Commun.*, vol. 203, pp. 66-82, 2016. doi:10.1016/j.cpc.2016.02.007
- [9] A. Bonatto *et al.*, “Passive and active plasma deceleration for the compact disposal of electron beams”, *Phys. Plasmas*, vol. 22, no. 8, p. 083106, 2015. doi:10.1063/1.4928379
- [10] R. I. Spitsyn and K. V. Lotov, “Wakefield decay in a radially bounded plasma due to formation of electron halo”, *Plasma Phys. Control. Fusion*, vol. 63, no. 5, p. 055002, 2021. doi:10.1088/1361-6587/abe055
- [11] K. V. Lotov, “Physics of beam self-modulation in plasma wakefield accelerators”, *Phys. Plasmas*, vol. 22, no. 10, p. 103110, 2015. doi:10.1063/1.4933129